Numerical modelling of a point-absorbing WEC model using DualSPHysics coupled with a multiphysics library

Bonaventura Tagliafierro, Alejandro J. C. Crespo, José M. Domínguez, Orlando García-Feal, Moncho Gómez-Gesteira, Ricardo B. Canelas, Ryan G. Coe, Giorgio Bacelli, Hancheol Cho, Steve J. Spencer, Giacomo Viccione

Abstract—**The aim of this work is to present the capabilities of the meshless numerical model named DualSPHysics, which coupled with a multiphysics library, is able to reproduce the interaction between waves and a floating wave energy converter (WEC). This is a challenging problem to be simulated with a numerical model since it includes not only the non-linear wave-structure interaction, but also the mechanical constraints of the floating WEC. DualSPHysics, which is a SPH-based code, is herein coupled with the Chrono library. This library is developed as a general-purpose simulation package for multi-body problems. The library is implemented under the DualSPHysics code, providing an integrated interface to define and run arbitrarily defined fluid–structure–structure coupled systems under the same framework. The DualSPHysics-Chrono coupled model was already validated for fluid–structure–structure interaction cases and it is here applied to simulate a floating point absorber. The model-scale WEC was designed and tested in MASK basin. The WEC is independently actuated in heave, surge, and pitch (all the degrees of freedom in a single plane). Tests have been conducted for the investigation of control to improve power generation and load reduction and to study system identification (SID) and model validation. Some of those tests are here reproduced with the proposed numerical tool. Numerical forces exerted by monochromatic waves onto the floating point absorber are compared with the experimental data and good agreement is observed. Therefore, DualSPHysics-Chrono is proposed as a design tool to improve the efficiency and survivability of this floating WEC, and could eventually be used to model the full PTO system, a challenging task for most CFD software.**

Keywords—**CFD, Chrono, Multiphysics, Numerical modelling, Point absorber, DualSPHysics.**

I. Introduction

In recent decades, wave energy has received significant attention for harnessing ocean energy. To this aim, present technology provides several harvesting devices such as bottom-hinged rotating systems, overtopping systems, oscillating water columns, and point absorbers. While each of these devices have unique characteristics, they are all subject to more or less the same physics (with overtopping devices being the main exception since they are not resonant devices).

A range of modeling approaches have been utilized to analyze WECs [1]-[2]-[3]. While the models used to perform numerical simulations of WEC dynamics in operational sea states are rather well understood, the task of simulating a WEC response in large sea states has not been studied nearly as much. Traditionally, models based on potential flow theory (see, e.g., [4]) have been used for modeling WECs in operation sea states. These models utilize a boundary element model (BEM) to solve for the frequency-dependent dynamics of arbitrary geometries [5]-[6]. Potential flow based models, which include both frequency domain models and time-domain models based on Cummins equation, such as WEC-Sim [7] and AQWA

1672-WHM

This work was supported in part by Xunta de Galicia under project "Programa de Consolidación e Estructuración de Unidades de Investigación Competitivas (Grupos de Referencia Competitiva) GRC2013-001" and under project "NUMANTIA ED431F 2016/004". The work is also financed by the Ministry of Economy and Competitiveness of the Government of Spain under project "WELCOME ENE2016-75074-C2-1-R". In addition, Sandia National Laboratories is a multi-mission laboratory managed and operated by National Technology and Engineering Solutions of Sandia, LLC., a wholly owned subsidiary of Honeywell International, Inc., for the U.S. Department of Energy's National Nuclear Security Administration under contract DE-NA0003525. This paper describes objective technical results and analysis. Any subjective views or opinions that might be expressed in the paper do not necessarily represent the views of the U.S. Department of Energy or the United States Government.

B. Tagliafierro, A. J. C. Crespo, J. M. Domínguez, O. García-Feal and M. Gómez-Gesteira are with the Environmental Physics Laboratory, Universidade de Vigo, Ourense, Spain (e-mail: btagliafierro@uvigo.es, alexbexe@uvigo.es, jmdominguez@uvigo.es, orlando@uvigo.es, mggesteira@uvigo.es).

R. B. Canelas is with the Instituto Superior Tecnico, Lisbon, Portugal (e-mail: ricardo.canelas@ist.utl.pt).

R. G. Coe, G. Bacelli, H. Cho and S. J. Spencer are with the Sandia National Laboratories, USA (email: rcoe@sandia.gov, gbacell@sandia.gov, hancho@sandia.gov, sjspenc@sandia.gov).

G. Viccione is with the University of Salerno, Italy (email: gviccion@unisa.it).

[8], are built upon a number of key assumptions. First, for potential flow, we assume the fluid to be both irrotational and inviscid. Next, to solve the BEM, we assume small amplitude motion and linear superposition.

It is clear to see how the assumptions of potential flow based models can be violated for a WEC, especially under energetic sea states. Thus, a growing number of studies have considered models based on the Reynolds Averaged Navier–Stokes (RANS) equations (see, e.g., [9,10,11,12]). However, due mainly to the complexities of modeling multiple moving bodies and modeling free surface waves, the application of these traditional Eulerian (mesh-based) methods is increasingly being reconsidering in exchange for newer meshless models. If the mesh-based approach solves the equations at fixed nodes in the space, in the meshless description, the positions where equations are solved move with the fluid and a fixed mesh is not used. The mesh-based methods (finite elements, finite differences and finite volumes) are currently very robust, well developed and have been applied to a wide range of applications providing highly accurate results. These mesh-based methods are ideal for systems where the domain is perfectly defined and for simulations where the boundaries remain fixed. However, the creation of the mesh can be very inefficient for complex systems.

In recent years, numerous meshless methods have appeared and grown in popularity as they can be applied to problems that are highly nonlinear in arbitrarily complex geometries and are difficult for mesh-based methods. Within the meshless methods now available, Smoothed Particle Hydrodynamics is, possibly, the most popular and has attained the required level of maturity to be used for engineering purposes. SPH describes a fluid by replacing its continuum properties with locally smoothed quantities at discrete Lagrangian locations named particles. Each of these particles is a nodal point for which physical quantities are computed as an interpolation of the values of the neighboring particles solving the Navier-Stokes equations. SPH is an ideal technique to simulate free-surface flows and presents several advantages compared with mesh-based methods to simulate violent wave-structure interaction. There is no special treatment to detect the free surface so large deformation can be efficiently treated since there is no mesh distortion. Other important advantage is that moving complex boundaries and interfaces are easily handled. The work of [13] is one the first examples of SPH modelling of point absorber devices.

The DualSPHysics open-source code ([14])–has been designed to use SPH for real engineering problems with software that can be run on either CPUs or GPUs (graphics cards with powerful parallel computing). GPUs offer now a higher computing power than CPUs and they are an affordable option to accelerate SPH with a low economic cost. Thereby, the simulations can be performed using a GPU card installed on a personal computer. Some simulations may require remarkably large domains and high resolution so that DualSPHysics is a perfect candidate since it is the most efficient SPH code worldwide ([15]). DualSPHysics has been recently coupled with Project Chrono, which is a library developed as a general-purpose simulation package for multi-body. The library is implemented under the DualSPHysics code, providing an integrated interface to define and run arbitrarily defined fluid–structure–structure coupled systems under the same framework. The DualSPHysics-Chrono coupled model was already validated [16] for fluid–structure–structure interaction cases and it is here applied to simulate the behavior of a floating point absorber. Therefore, the coupled model will be employed to simulate not only the interaction of waves with the floating device, but also the internal mechanical constraints and could eventually be used to model the full PTO system, a challenging task for most CFD software.

The model-scale WEC was designed and testing in the US Navy's Maneuvering And Sea Keeping (MASK) basin. The tested WEC is designed with the goal of better understanding WEC dynamics and controls. Additionally, the testing datasets from the wave tank tests of this device are freely available online at MHK-DR (https://mhkdr.openei.org).

The aim of this work is to validate the numerical model in order to propose it as a design tool to improve the efficiency and survivability of floating point absorbers. Section 2 gives some information about the WEC device and the experimental campaign. Section 3 describes, very briefly, the main governing equations of the SPH models and the functionalities of the DualSPHysics code to simulate the interaction of waves and floating structures. Section 4 shows the results of validation. The conclusions and future work are addressed in the last section.

II. EXPERIMENTAL DEVICE

The point absorber under study was tested in the MASK basin. This floating WEC is independently actuated in heave, surge, and pitch (all the degrees of freedom in 2D). Tests have been conducted for the investigation of control to improve power generation and load reduction and to study system identification (SID) and model validation. Tests include monochromatic waves, idealized ocean spectra, and multi-sine waves designed for SID.

Figure 1 shows the CAD model of the point absorber device tested in MASK basin [17]. The WEC has a major radius of 0.86 m, a draft of 0.53 m, and a displacement of 858 kg. Three permanent magnet electrical motors act as the device's PTOs. A "U-joint" located just below the device's centre of gravity to allow for pitch actuation. Belt drive transmissions are used to actuate the heave and

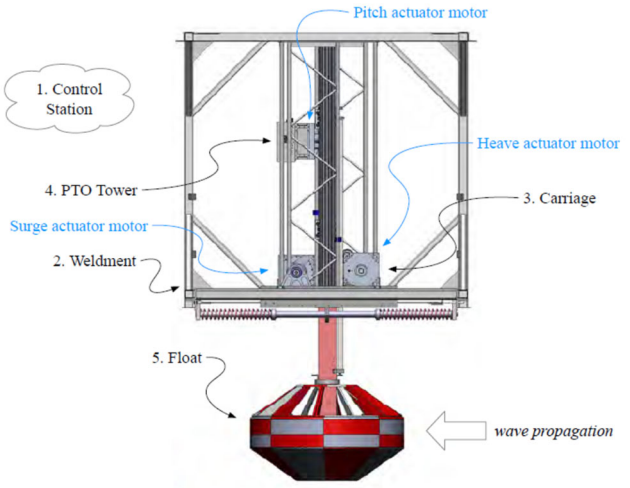

Fig. 1. CAD model of the point absorber device tested in US Navy's Maneuvering And Sea Keeping (MASK) basin [17].

surge degrees of freedom. Measurements of the system include motor torque and current, actuator force, accelerations, positions and orientations, and wave probes within the basin.

III. NUMERICAL MODELLING

The following sub-sections will briefly describe the SPH formulation implemented in DualSPHysics code and important functionalities that are required to simulate the interaction between waves and floating objects.

A. SPH basis

The Smoothed Particle Hydrodynamics (SPH) method uses particles to represent a fluid which move according to the governing dynamics. These particles are nodal points where physical quantities (e.g. position, velocity, density, pressure) are computed as an interpolation of the values of the neighboring particles. When simulating free-surface flows, the Lagrangian nature of SPH allows the domain to be multiply-connected, with no need of a special treatment of the surface, making the technique ideal for studying violent free-surface motion. SPH has been used to describe a variety of free-surface flows (wave propagation over a beach, plunging breakers, impact on structures and dam breaks).

The mathematical fundamental of SPH is based on integral interpolants. Any function F can be computed by the integral approximation:

$$F(\boldsymbol{r}) = \int F(\boldsymbol{r}')W(\boldsymbol{r}-\boldsymbol{r}',h)d\boldsymbol{r}' \qquad (1)$$

This function F can be expressed in a discrete form based on the particles. Thus, the approximation of the function is interpolated at particle a and the summation is performed over all the particles within the region of compact support of the kernel:

$$F(\boldsymbol{r_a}) \approx \sum_b F(\boldsymbol{r_b})W(\boldsymbol{r_a}-\boldsymbol{r_b},h)\frac{m_b}{\rho_b} \qquad (2)$$

where the volume associated to the neighboring particle b is m_b/ρ_b, with m and ρ being the mass and the density, respectively.

The kernel functions W must fulfil several properties ([18]), such as positivity inside the area of interaction, compact support, normalization and monotonically decreasing with distance. One option is the Quintic Wendland kernel [19]

$$W(q) = \alpha_D\left(1-\frac{q}{2}\right)^4(2q+1) \qquad 0 \le q \le 2 \qquad (3)$$

where $q=r/h$ is the normalized distance.

In the classical SPH formulation, the Navier-Stokes equations are solved and the fluid is treated as weakly compressible (WCSPH). The conservation laws of continuum fluid dynamics, in the form of differential equations, are transformed into their particle forms by the use of the kernel functions.

The momentum equation proposed by [18] has been used to determine the acceleration of a particle (a) as the result of the particle interaction with its neighbors (particles b):

$$\frac{d\boldsymbol{v}_a}{dt} = -\sum_b m_b\left(\frac{P_b+P_a}{\rho_b\cdot\rho_a}+\pi_{ab}\right)\nabla_a W_{ab} + \boldsymbol{g} \qquad (4)$$

being v velocity, P pressure, $\boldsymbol{g}$=(0,0,-9.81) ms^{-2} the gravitational acceleration and W_{ab} the kernel function that depends on the distance between particle a and b. The term π_{ab} is the viscous term according to the artificial viscosity proposed in [18].

The mass of each particle is constant, so that changes in fluid density are computed by solving the conservation of mass or continuity equation in SPH form:

$$\frac{d\rho_a}{dt} = \sum_b m_b\boldsymbol{v}_{ab}\nabla_a W_{ab} \qquad (5)$$

In the WCSPH, the fluid is treated as weakly compressible and Tait's equation of state is used to determine fluid pressure based on particle density. The compressibility is adjusted so that the speed of sound can be artificially lowered; this means that the time step can be maintained at a reasonable value.

The Symplectic time integration algorithm ([20]) was used in the present work and a variable time step was calculated, involving the CFL (Courant-Friedrich-Lewy) condition, the force terms and the viscous diffusion term.

B. *Floating bodies*

The movement of an object by considering its interaction with fluid particles and using these forces to drive its motion can be also derived in DualSPHysics. This can be achieved by summing the force contributions for an entire body. By assuming that the body is rigid, the net force on each boundary particle is computed according to the sum of the contributions of all surrounding fluid particles according to the designated kernel function and smoothing length. Each boundary particle k experiences a force per unit mass given by

$$\boldsymbol{f}_k = \sum_{a \in WPs} \boldsymbol{f}_{ka} \tag{6}$$

where $\mathbf{f}_{ka}$ is the force per unit mass exerted by the fluid particle *a* on the boundary particle *k*, which is given by

$$m_k \boldsymbol{f}_{ka} = -m_a \boldsymbol{f}_{ak} \tag{7}$$

For the motion of the moving body, the basic equations of rigid body dynamics can then be used

$$\begin{aligned} M\frac{d\boldsymbol{V}}{dt} &= \sum_{k \in BPs} m_k \boldsymbol{f}_k \\ I\frac{d\boldsymbol{\Omega}}{dt} &= \sum_{k \in BPs} m_k (\boldsymbol{r}_k - \boldsymbol{R}_0) \times \boldsymbol{f}_k \end{aligned} \tag{8}$$

where *M* is the mass of the object, *I* the moment of inertia, *V* the velocity, Ω the rotational velocity and R_0 the center of mass. Equation (8) are integrated in time in order to predict the values of *V* and Ω at the beginning of the next time step. Each boundary particle within the body has a velocity given by

$$\boldsymbol{u}_k = \boldsymbol{V} + \boldsymbol{\Omega} \times (\boldsymbol{r}_k - \boldsymbol{R}_0) \tag{9}$$

Finally, the boundary particles within the rigid body are moved by integrating (9) in time. The work in [21] showed that this technique conserves both linear and angular momentum.

Validations about buoyancy-driven motion are performed in [22], where DualSPHysics was tested for solid objects larger than the smallest flow scales and with various densities. Simulations are compared with analytical solutions, other numerical methods and experimental measurements. Moreover, simulations of a floating box under the action of regular waves were also compared with experimental data in [23] where a good agreement was observed between numerical and experimental heave and surge motions and pitch rotation.

C. *Wave generation*

Long-crested waves are generated in DualSPHysics by means of moving boundaries that mimic the movement of a wavemaker as in physical facilities. The wave generation using moving boundary in DualSPHysics consists of piston- and also flap-type wavemakers. A piston-type wavemaker is used in the present study. First and second order wave generation theories are implemented in DualSPHysics. The first order generation is fully described in [24], where generation methods for both monochromatic and random waves are reported. For second order wave generation of monochromatic waves, the reader is referred to the solution proposed by [25]. The first order wave generation for monochromatic waves is extended to random waves in DualSPHysics based on the method described in [26]. Two standard wave spectra are implemented and used to generate random waves: JONSWAP and Pierson-Moskowitz spectra. In this way, wave height, wave period and depth are the key input parameters in DualSPHysics, therefore the time series of wavemaker displacement is computed using the aforementioned wave theory.

D. *Passive wave absorption*

The use of wave absorption allows generating long time series of sea waves in relatively short domains with negligible wave reflection. The passive wave absorption consists of a damping system at the end of the domain that reduces the wave energy (i.e. wave height and period). This system can be either a dissipative beach or a "sponge" area: both have been implemented and checked in DualSPHysics. A dissipative beach is usually a kind of passive absorption system that is used in physical model tests. Dissipative beaches are systems where most wave energy is expended through the process of breaking. The beach can have a straight or parabolic shape. The former one is implemented in DualSPHysics, where the angle of the beach with respect to the horizontal is constant.

The sponge area reduces the velocity of the particles following $\mathbf{v}=\mathbf{v}_0 \cdot f(x,dt)$, where $\mathbf{v}_0$ is the initial velocity of the particle *i* that enter this area, $\mathbf{v}$ is the final velocity and $f(x,dt)$ is the reduction function defined following [24] as:

$$f(x, dt) = 1 - dt \cdot \beta \cdot \left(\frac{x - x_0}{x_1 - x_0}\right)^2 \tag{10}$$

where dt is the duration of the last time step, x is the position of the particles, x_0 and x_1 are the initial and final position of the sponge area, respectively.

E. *Active wave absorption for piston-type wavemaker*

Active wave absorption is used in physical facilities to absorb the reflected waves at the wavemaker in order to avoid that they will be reflected back into the domain. In this way, the active absorption prevents the introduction into the system of extra spurious energy that will bias the results.

The active wave absorption system (AWAS) has been implemented in DualSPHysics for a piston-type wavemaker. The technique is based on the approach that appears in [27]. The water surface elevation η at the wavemaker position is used and transformed by an

appropriate time-domain filter to obtain a control signal that corrects the piston displacement in order to absorb the reflected waves every time step.

Hence, the wavemaker displacement is corrected to avoid further reflection at the wavemaker. The position in real time of the wavemaker is obtained through the velocity correction of its motion. For a piston-type wavemaker the velocity correction is calculated using linear long wave theory in shallow water ([27]). The method requires to estimate the free-surface elevation of the reflected waves, η_R, to be absorbed comparing the target incident water surface elevation, η_I, with the measured one in front of the wave-maker, η_{SPH}. The corrected wavemaker velocity is then the summation of velocity correction and the theoretical incident wave-maker velocity. For further details about the implementation of AWAS in DualSPHysics, the reader is referred to [24].

F. Coupling with multiphysics library (Chrono)

In order to take into account the mechanical restrictions applied on the rigid body, a Project Chrono (https://projectchrono.org/) implementation is used. The coupling allows for arbitrarily shaped bodies to be considered, and the solver is capable of integrating externally applied forces and torques (the resultants of the fluid-body interactions) and the effects of kinematic-type restrictions, dynamic-type restrictions and internal collisions, as shown in [16]. The problem is described using a Differential Variational Inequality (DVI), cast in Cone Complementary Problem (CCP) form and solved with a novel fixed point iterative method [28]. This allows for high accuracy and computational efficiency.

IV. RESULTS

As mentioned before, the tests of the floating point absorber in the MASK basin include monochromatic waves and irregular waves. In addition, large waves, resulting in overtopping and slamming were included in the experimental tests. As a first step, the tests of monochromatic waves are used in this work for validation purposes. Therefore, the cases with regular waves are simulated with the DualSPHysics-Chrono model in order to obtain the numerical forces exerted onto the WEC. Finally, the force time series are compared with the experimental ones. Tests with reference 005, 006 and 009 in [17] are herein considered. Note that only one degree of freedom (heave motion) was activated in those tests; the WEC was constrained to slide only vertically and no external attenuator was applied.

Table 1 collects the wave conditions of these three tests, including the wave period (T), the wave height (H), wavelength (L) and water depth in the basin (d_B) and depth of the numerical tank (d_N).

TABLE I
WAVE CONDITIONS

	Case 1	Case 2	Case 3
Ref. in [17]	009	006	005
T [s]	1.11	1.25	1.43
H [m]	0.085	0.080	0.085
L [m]	1.92	2.43	3.17
d_B *[m]*	6.10	6.10	6.10
d_N *[m]*	1.00	1.20	1.50

Figure 2 shows the numerical domain; wave flume and WEC device. The size of this numerical flume is much smaller than the experimental MASK basin [16], however the dimensions of the point absorber are exactly the same. Reductions in length, width and depth took place but wave conditions remain to follow the tested ones in the basin. These reductions are necessary due to the high computational cost of the numerical model. The length of the domain includes a flat region of 5 m (higher than the maximum wavelength to guarantee a correct wave propagation as suggested in [24]) and 2 m length of a dissipative beach (slope of 45°). A sponge layer (following (10)) is also applied in the region of the beach to remove any possible wave reflection. The width of the flume corresponds to more than twice the WEC diameter. Note that the work of [29] suggested that flume width should be 3-5 times higher than WEC size to reduce side wall reflection, so lateral sponge layers have been included in the simulation to keep the value of width as low as possible but minimizing lateral reflection. The depth of the numerical tank (d_N) is much smaller than the depth of the basin (d_B). Even with the reduction in depth, the wave propagation conditions shown in Table 1 still correspond to deep water.

In addition, the piston-type wavemaker generates waves in the numerical domain along with the AWAS to absorb reflected waves from the device. The movement of the piston is automatically computed by DualSPHysics to create the incident waves of Table 1.

Finally, the floating WEC is created as a set of boundary particles (DBC) that form part of the same rigid body and are moved following both (9) and the mechanical constraints defined in the Chrono library. In this case the internal mechanical constraints restrict the degrees of freedom to only heave motion, since in the experiments (used herein for validation) the floating point absorber can only oscillate in vertical direction. The center of the floating WEC is located at 4 m from the piston, which is longer than the maximum value of the wavelengths in Table 1.

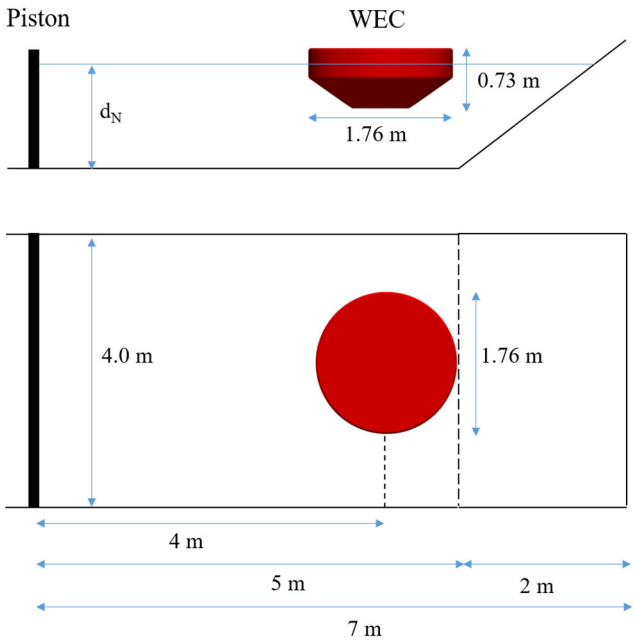

Fig. 2. Numerical domain: dimensions of the wave flume and point absorber (cross section and top view).

Despite of the reductions applied to the numerical tank, in order to mimic the MASKIN basin, the number of particles can still be large with fine resolution. As suggested in [24], the minimum number of particles to discretize one wave height (H) should be 5. For an initial inter-particle spacing of dp = 0.015 m, then H/dp=5.66 (so the minimum off 5 is fulfilled). Table 2 includes the total number of generated particles (Np) and the runtime for the three simulations (the three wave conditions in Table 1) for 20 seconds of physical time. The number of particles increases with the numerical depth (d_N). Total runtimes are obtained using the GPU Tesla k40 as execution device.

TABLE II
NUMBER OF PARTICLES AND RUNTIMES OF THE DIFFERENT CASES

	Case 1	Case 2	Case 3
Ref. in [17]	009	006	005
dp	0.015	0.015	0.015
Np	6,433,499	7,756,583	10,194,207
Runtime	156 h	220 h	291 h

Initially, a numerical domain without the WEC was considered to check that the incident waves were properly generated and propagated until the location of the device. The three regular wave conditions of Table 1 were simulated and free-surface elevations were computed at 4 m, which is the distance between the piston and the location where the center of the device would be located. Figure 3 compares the numerical free-surface elevation with the theoretical value using Stokes' 2nd order theory. A good agreement is achieved in the three cases so waves are being generated and propagated with accuracy. Some discrepancies can be observed for the Case 1 (the case with the lowest wave period), however the difference is smaller than the initial particle spacing (dp), which can be considered here as the numerical error ([24]). Following these results, we can conclude that the modifications in the tank (reducing length, depth and width) are acceptable to perform simulations with less particles than needed in the real experimental case.

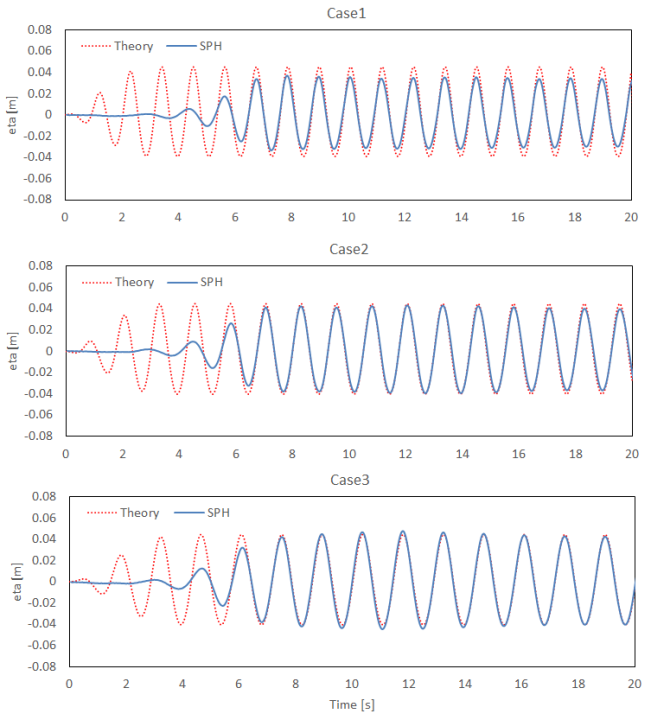

Fig. 3. Comparison of theoretical (Stokes' 2nd order) and numerical (DualSPHysics) free-surface elevation at 4 m from the piston.

Next, the results of the simulations including the floating WEC in numerical flume are analyzed. Several time instants of the simulation of Case 3 (Table 1) using the coupled DualSPHysics-Chrono model can be observed in Figure 4. For a better visualization a vertical tube is included in the images to represent the experimental constraint since the floating WEC can only oscillate in the vertical direction (only heave motion). The color of the fluid surface corresponds to horizontal velocity to show how waves propagate from the piston to the device.

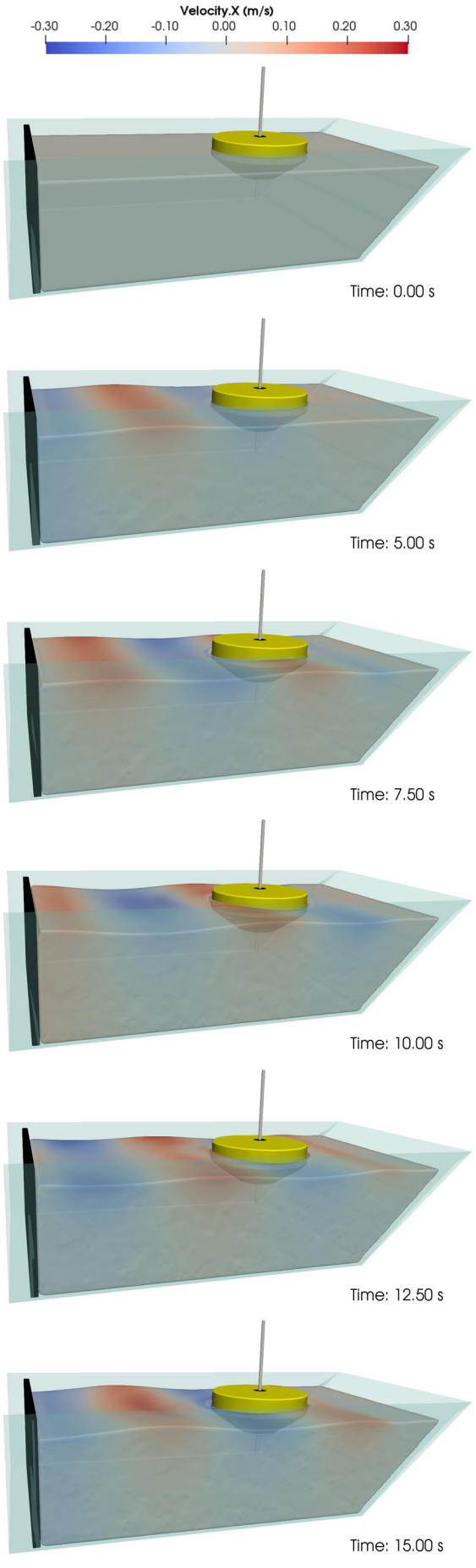

Fig. 4. Different instants of the numerical simulation of Case3.

The wave period is the main parameter that governs the vertical forces exerted onto the WEC. Figure 5 compares the experimental [17] and the numerical vertical forces for the three cases. A very good agreement is observed for Cases 1 and 2. Some differences appear in the comparison for Case 3, where the experimental peaks include higher order components that are not reproduced in the numerical model. This could be related with the numerical resolution (dp=0.015 m) since we are using the minimum suggested resolution (following [24]) to get proper wave propagation. However, authors of the experiments observed that the higher order effects are likely due to some issues in the mechanical arrangement in the physical tests.

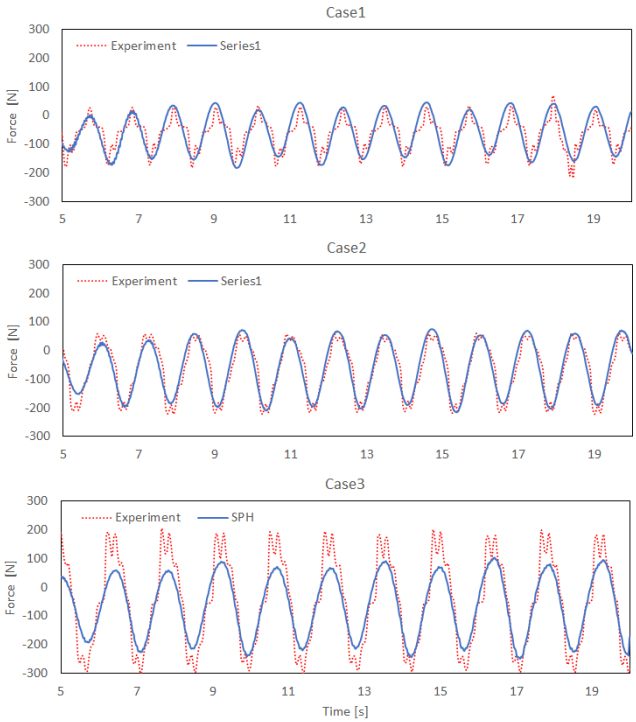

Fig. 5. Comparison of experimental ([17]) and numerical (DualSPHysics) vertical forces exerted onto the point absorber (restricted to only heave motion).

V. Conclusion

In this work the coupling between the DualSPHysics code with the Project Chrono library was validated by describing the motion of a floating point absorber. Nonlinear constraints are considered to simulate the effect of mechanical systems. The numerical model can predict, with a satisfactory accuracy, the vertical oscillation of the floating device under the action of regular waves. The numerical results of the vertical force exerted onto the WEC show a good agreement with experimental data. Therefore, DualSPHysics-Chrono coupled model can be employed to simulate the interaction of waves with the floating device, as well as the internal mechanical constraints. Eventually, this tool could be used to model the full PTO system, a challenging task for most CFD software. The numerical model can be proposed as a design tool to improve the efficiency and survivability of this floating WEC under high energetic sea states.

REFERENCES

[1] Y. Li, Y.-H Yu, "A synthesis of numerical methods for modeling wave energy converter-point absorbers," *Renewable and Sustainable Energy Reviews*, vol. 16, no. 6, pp. 4352-4364, 2012.

[2] M. Folley, et al. "A review of numerical modelling of wave energy converter arrays," *ASME 2012 31st International Conference on Ocean, Offshore and Arctic Engineering*, American Society of Mechanical Engineers, 2012.

[3] P. Markel, and J. Ringwood. "A review of wave-to-wire models for wave energy converters," *Energies 9.7*, vol. 506, 2016.

[4] J. N. Newman, "Marine hydrodynamics", *MIT press*, 2018.

[5] C-H. Lee, "WAMIT theory manual", *Massachusetts Institute of Technology*, Department of Ocean Engineering, 1995.

[6] B. Aurélien, G. Delhommeau. "Theoretical and numerical aspects of the open source BEM solver NEMOH," *11th European Wave and Tidal Energy Conference (EWTEC2015)*, 2015.

[7] M. Lawson et al., "Development and demonstration of the WEC-Sim wave energy converter simulation tool," 2014.

[8] ANSYS, AQWA. "Version 15.0; ANSYS" Inc.: Canonsburg, PA, USA November, vol. 752,2013.

[9] R.G. Coe, B.J. Rosenberg, E.W. Quon, C.C. Chartrand, Y-H. Yu, J. van Rij, T.R. Mundon, "CFD design load analysis of a two-body wave energy converter," *Journal of Ocean Engineering and Marine Energy*, in press.

[10] J. Westphalen, M.D. Greaves, A. Raby, Z.Z. Hu, D.M. Causon, C.G. Mingham, P. Omidvar, P.K. Stansby, D.B. Rogers, "Investigation of wave-structure interaction using state of the art CFD techniques", *Open Journal of Fluid Dynamics*, vol. 04, no. 01, pp.18–43, 2014, DOI> 10.4236/o jfd.2014.41003

[11] Y.H. Yu, Y. Li, "Reynolds-averaged Navier-Stokes simulation of the heave performance of a two-body floating-point absorber wave energy system", *Computers and Fluids*, 2013, vol. 73, pp. 104–114, DOI: 10.1016/j.compfluid.2012.10.007

[12] E. Ransley, D. Greaves, A. Raby, D. Simmonds, MM. Jakobsen, "Kramer M (2017b) RANS-VOF modelling of the Wavestar point absorber". *Renewable Energy*, vol. 109, pp. 49–65, 2017.

[13] S. Yeylaghi, B. Moa, S. Beatty, B. Buckham, P. Oshkai, C. Crawfoed, "SPH Modeling of Hydrodynamic Loads on a Point Absorber Wave Energy Converter Hull", in *Proceedings of the 11th European Wave and Tidal Energy Conference (EWTEC2015)*, Nantes, France, 2015.

[14] A. J. C. Crespo, J. M. Domínguez, B. D. Rogers, M. Gómez-Gesteira, S. Longshaw, R. Canelas, R. Vacondio, A. Barreiro, O. García-Feal, "DualSPHysics: open-source parallel CFD solver on Smoothed Particle Hydrodynamics (SPH)", *Computer Physics Communications*, vol. 187, pp. 204-216, 2015.

[15] J. M. Domínguez, A. J. C. Crespo, B. Valdez-Balderas, B. D. Rogers, M. Gómez-Gesteira, "New multi-GPU implementation for Smoothed Particle Hydrodynamics on heterogeneous clusters", *Computer Physics Communications*, vol. 184, pp. 1848-1860, 2013.

[16] R.B.C. Canelas, A.J.C. Crespo, M. Brito, J.M. Domínguez, O. García-Feal, "Extending DualSPHysics with a Differential Variational Inequality: modeling fluid-mechanism interaction", *Applied Ocean Research*, vol.76, pp. 88-97, 2018.

[17] R.G. Coe, G. Bacelli, S.J. Spencer, H. Cho, "Initial results from wave tank test of closed-loop WEC control" *Sandia National Laboratories*, report SAND2018-1258, 2018.

[18] J. J. Monaghan, "Smoothed particle hydrodynamics", *Annual Review of Astronomy and Astrophysics*, vol. 30, pp. 543-574, 1992.

[19] H. Wendland, "Piecewiese polynomial, positive definite and compactly supported radial functions of minimal degree", *Advances in Computational Mathematics*, vol. 4, pp. 389-396, 1995.

[20] B. J. Leimkuhler, S. Reich, R. D. Skeel, "Integration Methods for Molecular dynamic IMA", *Volume in Mathematics and its application*. Springer, 1996.

[21] J. J. Monaghan, A. Kos, A. Issa, "Fluid motion generated by impact", *Journal of Waterway Port, Coastal and Ocean Engineering*, vol. 129, pp. 250-259, 2003.

[22] R. B. Canelas, J. M. Domínguez, A. J. C. Crespo, M. Gómez-Gesteira, R. M. L. Ferreira, "A Smooth Particle Hydrodynamics discretization for the modelling of free surface flows and rigid body dynamics", *International Journal for Numerical Methods in Fluids*, vol. 78, pp. 581-593, 2015.

[23] A. J. C. Crespo, J. M. Domínguez, M. Gómez-Gesteira, M. Hall, C. Altomare, M. Wu, T. Verbrugghe, V. Stratigaki, P. Troch, D. Kisacik, I. Simonetti, L. Cappietti, R. B. Canelas, R. M. L. Ferreira, P. Stansby, "Survivability of floating moored offshore structures studied with DualSPHysics*", in Proceedings of the 13th SPHERIC International Workshop*, 2018, Galway, Ireland.

[24] C. Altomare, T. Suzuki, J. M. Domínguez, A. Barreiro, A. J. C. Crespo, M. Gómez-Gesteira, "Numerical wave dynamics using Lagrangian approach: wave generation and passive & active wave absorption*", in Proceedings of the 10th SPHERIC International Workshop*, 2015, Parma, Italy.

[25] O. S. Madsen, "On the generation of long waves", *Journal of Geophysical Research*, vol. 76, no.36, pp. 8672–8683, 1971.

[26] Z. Liu, P. Frigaard, "Generation and Analysis of Random Waves". *Laboratoriet for Hydraulik og Havnebygning*, Instituttet for Vand, Jord og Miljoeteknik, Aalborg Universitet, 2001.

[27] H. A. Shaffer, G. Klopman, "Review of Multidirectional Active Wave Absorption Methods", *Journal of Waterway, Port, Coastal and Ocean Engineering*, vol. 126, pp. 88-97, 2000.

[28] A. Tasora, M. Anitescu, "A matrix-free cone complementarity approach for solving large-scale", *Nonsmooth Rigid Body Dyn.*, vol. 200, no. 5, pp. 439–453, 2011.

[29] S.K. Chakrabarti, "Modeling Laws in Ocean Engineering". in *Developments in Offshore Engineering, wave phenomena and offshore topic', Herbich, J.B (Ed)*, ch. 7, 1999, Gulf Publishing Company, Texas.